Dynamical formation of the Bose polaron through impurity-bath decoherence

K. K. Nielsen,[1] L. A. Peña Ardila,[1] G. M. Bruun,[1] and T. Pohl[1]

[1]*Department of Physics and Astronomy, Aarhus University, Ny Munkegade, DK-8000 Aarhus C, Denmark*

(Dated: May 23, 2022)

We study the quantum dynamics of a single impurity following its sudden immersion into a Bose-Einstein condensate. The formation of the Bose polaron after such a quench stems from decoherence of the impurity, driven by collisions with the condensate. Using a master equation approach, we derive rigorous analytical results for the decoherence dynamics of the impurity, which reveals different stages of its evolution from a universal non-exponential initial relaxation to the final approach of the equilibrium state of the Bose polaron. The associated polaron formation time exhibit a strong dependence of the impurity momentum and is found to undergo a critical slowdown around the Landau critical velocity of the condensate. The rich non-equilibrium behavior of quantum impurities in a Bose gas revealed in this work is of direct relevance to recent cold-atom experiments, in which Bose polarons are created by a sudden quench of the impurity-bath interaction.

I. INTRODUCTION

Understanding the non-equilibrium dynamics of many-body systems remains one of the most outstanding challenges in physics. Cold atomic gases have emerged as an excellent platform to explore this question [1], since they can be well isolated from their environment and offer an extraordinary level of control. In particular, the precise tunability of interactions through Feshbach resonances [2–4] has opened the door to studies of interaction effects in quantum many-body systems with unprecedented control. While this offers unique perspectives for studying paradigmatic models in condensed matter physics [5, 6], the scope of cold-atom research has extended well beyond such initial ideas. Exciting new research directions include the dynamical emergence of thermal equilibrium in isolated quantum systems [1], and the observation of many-body localization [7], linked to the breakdown of ergodicity [8, 9]. Another example is the polaron quasiparticle, which was originally introduced by Landau [10] to describe the interaction of electrons with the atomic crystal of a solid, and has since been employed to understand a broad range of problems in condensed matter physics [11]. Experiments on ultracold Fermionic atoms provide an ideal quantum simulation platform for this problem [12–16] enabling precise studies of the Fermi-polaron [17–19]. At the same time, the possibility to realize so-called Bose polarons in atomic Bose-Einstein condensates (BECs) [20, 21] has raised further questions and ushered in new theoretical investigations [22–33], expanding our understanding of quantum impurity physics. While much of previous efforts have been directed towards the equilibrium properties of the Bose polaron, its dynamics has spawned theoretical work only recently [34–39], predicting the formation of phonon-impurity bound states for strongly interacting systems [34] and studying trajectories and momentum relaxation of moving impurities [35–38], as well as the dynamics of phonon dressing in spinor condensates [39].
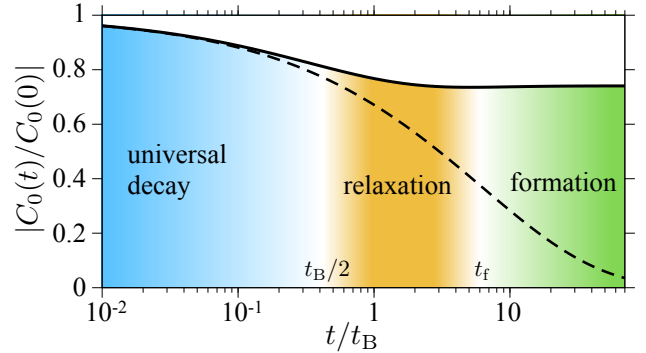

FIG. 1. Non-equilibrium dynamics of the coherence of a quantum impurity immersed in a Bose-Einstein condensate. The two timescales t_B and t_f define three evolution stages, from an initial universal coherence decay and an intermediate relaxation stage to the final formation of the polaron in which the absolute value of the coherence $|C_p|$ approaches the residue Z_p of the equilibrium polaron state, as shown by the black line for a boson-boson scattering length of $a_\mathrm{B}/\xi = 0.01$ and an impurity at rest with a scattering length $a/\xi = 0.1$ in the equal mass case $\alpha = m/m_\mathrm{B} = 1$. The dashed line shows the corresponding dynamics for a noninteracting BEC in which the universal initial decay $|C_p(t)| = |C_p(0)| \exp(-\sqrt{t/t_0})$, set by a third characteristic timescale t_0, persists throughout the entire time evolution of the quantum impurity.

Here we investigate the non-equilibrium dynamics of a mobile impurity in a BEC and reveal distinct evolution stages with associated timescales that determine the formation dynamics of the Bose polaron from an initial interaction quench to its final equilibrium steady state. Treating the BEC as a bath, we use a master equation approach for such a systematic characterization and derive rigorous results in the limit of weak impurity-boson interactions. Within this picture, the Bose polaron emerges as a consequence of impurity-bath decoherence, whereby all many-body states apart from the polaron ground state dephase as the phonon-dressed impurity approaches the known equilibrium state of the Bose polaron. As illustrated in Fig. 1, we identify three distinct stages and

corresponding timescales of the non-equilibrium impurity dynamics. The initial coherence of the impurity decays in a universal non-exponential fashion on a timescale that solely depends on the impurity-boson coupling. The subsequent relaxation however is strongly influenced by the boson-boson interaction, initiating the phonon dressing of the impurity. While the impurity eventually reaches its equilibrium polaron state [34], we find that the final polaron formation undergoes a critical slowdown as the impurity speed approaches the Landau critical velocity of the BEC. The determined characteristic timescales for polaron formation are within the resolution of current experiments, and should thus be observable in future measurements.

II. THE SYSTEM

We consider an impurity of mass m in a gas of bosons with a mass m_B and a density n_B. The boson-boson and boson-impurity interactions are both of short range nature and characterised by the scattering lengths a_B and a, respectively. For weak interactions and close to zero temperature, the bosons form a BEC that is accurately described by Bogoliubov theory [40]. The Hamiltonian,

$$H = H_B + H_I + H_{IB}, \qquad (1)$$

of this system can be separated into three terms, where

$$H_B = \sum_{\mathbf{k}} E_{\mathbf{k}} \beta_{\mathbf{k}}^\dagger \beta_{\mathbf{k}} \qquad (2)$$

describes the BEC in terms of Bogoliubov modes with momenta $\mathbf{k}$ and associated energies $E_{\mathbf{k}} = [\varepsilon_{\mathbf{k}}^B(\varepsilon_{\mathbf{k}}^B + 2n_B\mathcal{T}_B)]^{1/2}$ that are created by the operators $\beta_{\mathbf{k}}^\dagger$. Here, $\mathcal{T}_B = 4\pi a_B/m_B$ is the scattering matrix for the boson-boson interaction, and $\varepsilon_{\mathbf{k}}^B = k^2/2m_B$ is the bare boson kinetic energy at momentum $\mathbf{k}$. We work in units where $\hbar = 1$. The impurity Hamiltonian is given by

$$H_I = \sum_{\mathbf{k}} \varepsilon_{\mathbf{k}} c_{\mathbf{k}}^\dagger c_{\mathbf{k}}, \qquad (3)$$

where $c_{\mathbf{k}}^\dagger$ creates an impurity with momentum $\mathbf{k}$ and energy

$$\varepsilon_{\mathbf{k}} = k^2/2m + \varepsilon_{MF}, \qquad (4)$$

which includes the mean-field shift $\varepsilon_{MF} = n_B U_0$ of the impurity energy due to its interaction with the BEC. Here, $U_{\mathbf{k}}$ is the impurity-boson interaction momentum space. Accordingly the term

$$H_{IB} = \sum_{\mathbf{k},\mathbf{p}} U_{\mathbf{k}} \sqrt{\frac{n_B \varepsilon_{\mathbf{k}}^B}{V E_{\mathbf{k}}}} c_{\mathbf{p}-\mathbf{k}}^\dagger c_{\mathbf{p}} \left(\beta_{\mathbf{k}}^\dagger + \beta_{-\mathbf{k}} \right), \qquad (5)$$

describes the impurity-boson interaction. Eqs. (2)-(5) correspond to the so-called Fröhlich model [41], originally put forth to describe the electrons coupled to optical phonons of a dielectric crystal. In the present case

of an impurity in a BEC, there are interaction terms not included in Eq. (5), which describe the scattering of the impurity on bosons already excited out of the BEC. For small impurity-boson interactions, their contribution is, however, suppressed by a factor $(n_B a_B^3)^{1/2}$ [28], which we assume to be small. Focussing our analysis to the regime of validity of the Fröhlich Hamiltonian, we consider all observables to second order in the impurity scattering length a. Explicitly, we express the interaction as $U_{\mathbf{k}} = U_0 g_{\mathbf{k}}$, with $g_{\mathbf{k}}$ a rescaled coupling and $g_0 = 1$. We then solve the Lippmann-Schwinger equation to express U_0 in terms of a to second order. This yields $U_0 = \mathcal{T} + \mathcal{T}^2/(2\pi)^3 \int \mathrm{d}^3 k\, g_{\mathbf{k}}^2\, 2m_r/k^2$. Here $\mathcal{T} = 2\pi a/m_r$ is the zero energy impurity-boson scattering matrix and $m_r = m_B m/(m + m_B)$ denotes the reduced mass. This allows to re-express our results in terms of the scattering length a, which yields well-defined result in the limit of a zero range interaction, i.e. a momentum independent impurity-boson interaction with $g_{\mathbf{k}} = 1$. We however retain a momentum dependent $g_{\mathbf{k}}$ in the formalism in order to analyse how a small but finite interaction range can affect the initial impurity dynamics at early times.

In order to study decoherence, we consider a quench in which an impurity with momentum p is suddenly immersed into the condensate at time $t = 0$, creating the initial state

$$|\psi_0\rangle = \left(\cos\theta + \sin\theta c_{\mathbf{p}}^\dagger\right) |BEC\rangle, \qquad (6)$$

where θ is the mixing angle that determines the probability, $\sin^2\theta$, for initial impurity creation. The coherence between the vacuum and the single-impurity state can then be obtained from

$$C_p(t) = \langle \psi_0 | c_{\mathbf{p}}(t) | \psi_0 \rangle, \qquad (7)$$

where $c_{\mathbf{p}}(t) = \exp(iHt) c_{\mathbf{p}} \exp(-iHt)$ is the time-dependent impurity operator in the Heisenberg picture. The evolution of $C_p(t)$ closely traces the dynamical formation of the polaron, as we shall discuss in the rest of the paper.

Substituting the initial state Eq. (6)

$$C_p(t) = \cos\theta \sin\theta \langle BEC | c_{\mathbf{p}}(t) c_{\mathbf{p}}^\dagger(0) | BEC \rangle$$
$$= i \cos\theta \sin\theta G_{\mathbf{p}}(t), \qquad (8)$$

shows that the coherence is related to the time-dependent impurity Green's function, $G_{\mathbf{p}}$, for $t > 0$, and which also corresponds to the dynamical overlap considered in [34]. For long times, it should thus approach the asymptotic Greens function of the polaron

$$\lim_{t \to \infty} C_p(t) \sim Z_p e^{-iE_p \cdot t - t/2\tau_p}, \qquad (9)$$

and thereby define the polaron energy, E_p, the polaron lifetime τ_p, and the quasiparticle residue Z_p. For an infinite polaron lifetime, $|C_p(t)|$ therefore converges to the quasiparticle weight Z_p, as also found in [34].

In cold-atom experiments, the initial state Eq. (6) can be prepared by driving a transition between internal atomic states of the impurity which feature different

interactions. Indeed recent experimental demonstrations of the Bose polaron were based on RF spectroscopy on a hyperfine transition between a weakly and a strongly interacting state of a single-component ^{39}K BEC [20] or of ^{40}K impurity atoms immersed in a ^{87}Rb condensate [21]. In both cases, a direct measurement of the coherence dynamics is possible via Ramsey spectroscopy [42–44].

III. MASTER EQUATION DESCRIPTION

We determine the dynamics of the coherence using the impurity density operator ρ_I. First, we consider the density operator $\rho(t)$ of the entire system, i.e. the impurity and the BEC. In the interaction picture, it obeys the von Neumann equation

$$i\partial_t \rho = [H_\text{IB}(t), \rho(t)]. \tag{10}$$

One can formally solve this equation by integrating both sides and resubstituting the result into the right hand side of (10) to obtain

$$\partial_t \rho = -i[H_\text{IB}(t), \rho(0)] - \int_0^t \mathrm{d}s [H_\text{IB}(t), [H_\text{IB}(s), \rho(s)]]. \tag{11}$$

We can now trace out the bosonic degrees of freedom on both sides of Eq. (11) to obtain an evolution equation for the reduced density operator, $\rho_\text{I} = \text{Tr}_\text{B}\rho$, of the impurity. For our chosen initial state Eq. (6) the initial density operator of the entire system factorizes according to $\rho(0) = \rho_\text{I}(0) \otimes \rho_\text{B}(0)$, where $\rho_\text{B}(0) = |\text{BEC}\rangle \langle \text{BEC}|$ is the density operator for the BEC. Taking the trace of the first term in Eq. (11) only yields terms proportional to $\langle \beta \rangle = \langle \beta^\dagger \rangle = 0$, such that we obtain the following equation of motion for the impurity density operator

$$\partial_t \rho_\text{I} = -\int_0^t \mathrm{d}s\, \text{Tr}_\text{B}[H_\text{IB}(t), [H_\text{IB}(s), \rho_\text{I}(s) \otimes \rho_\text{B}(0)]]. \tag{12}$$

Here, we have made the Born approximation, $\rho(s) = \rho_\text{I}(s) \otimes \rho_\text{B}(0)$ assuming that the density matrix of the BEC is unaffected by the impurity, which is justified for small impurity interactions. In the same limit we can also replace $\rho_\text{I}(s)$ by $\rho_\text{I}(t)$ to obtain a time-local equation that contains all relevant contributions up to second order in the interaction strength [45, 46]. Altogether this makes it possible to evaluate the trace over the commutator in Eq. (12). Using further that $\langle \text{BEC}| \beta_\mathbf{k} \beta_{\mathbf{k}'}^\dagger |\text{BEC}\rangle = \delta_{\mathbf{k},\mathbf{k}'}$ and $\beta_\mathbf{k}(t) = \mathrm{e}^{-iE_\mathbf{k}t}\beta_\mathbf{k}(0)$ in the interaction picture, we finally obtain

$$\partial_t \rho_\text{I} = -\frac{n_\text{B}\mathcal{T}^2}{V} \sum_{\mathbf{k},\mathbf{p}1,\mathbf{p}2} g_\mathbf{k}^2 \frac{\varepsilon_\mathbf{k}^\text{B}}{E_\mathbf{k}} \int_0^t \mathrm{d}s \left(e^{-iE_\mathbf{k}(t-s)} \right.$$
$$\left. \times \left[c_{\mathbf{p}1-\mathbf{k}}^\dagger(t)c_{\mathbf{p}1}(t), c_{\mathbf{p}2+\mathbf{k}}^\dagger(s)c_{\mathbf{p}2}(s)\rho_\text{I}(t) \right] + \text{h.c.} \right). \tag{13}$$

Further details of this derivation are given in App. A. Equation (13) constitutes an effective von Neumann equation for the impurity density operator, and will now be used to determine the dynamics of the impurity coherence.

IV. IMPURITY COHERENCE

Knowing the time dependent density operator of the impurity we can calculate its coherence from

$$C_p(t) = \text{Tr}[c_\mathbf{p}(t)\rho_\text{I}(t)] = \langle 0| c_\mathbf{p}(t)\rho_\text{I}(t) |0\rangle, \tag{14}$$

where we now trace over the impurity degrees of freedom, and have used that only the vacuum $|0\rangle$ contributes to the trace for the initial state Eq. (6). It turns out to be convenient to introduce the coherence $\tilde{C}_p(t) = \mathrm{e}^{i\varepsilon_\mathbf{p}t}C_p(t)$, stripped of the single particle and mean field phase rotation. Using Eq. (14) and $c_\mathbf{p}(t) = \mathrm{e}^{-i\varepsilon_\mathbf{p}t}c_\mathbf{p}(0)$ we can write for its time evolution $\partial_t\tilde{C}_p(t) = \langle 0| c_\mathbf{p}(0)\partial_t\rho_\text{I}(t) |0\rangle$, which, upon substituting Eq. (13) and after some algebra, yields

$$\partial_t\tilde{C}_p(t) = i[\Gamma_p(t) - \Gamma_p(0)]\tilde{C}_p(t), \tag{15}$$

with the time dependent rate coefficient

$$\Gamma_p(t) = n_\text{B}\mathcal{T}^2 \int \frac{\mathrm{d}^3k}{(2\pi)^3} g_\mathbf{k}^2 \frac{\varepsilon_\mathbf{k}^\text{B}}{E_\mathbf{k}} \frac{\mathrm{e}^{i(\varepsilon_\mathbf{p}-\varepsilon_{\mathbf{p}-\mathbf{k}}-E_\mathbf{k})t}}{\varepsilon_\mathbf{p} - \varepsilon_{\mathbf{p}-\mathbf{k}} - E_\mathbf{k}}. \tag{16}$$

Equation (15) implies a pure decay of the impurity coherence driven by its interaction with the surrounding BEC. Indeed, population redistribution to other impurity momenta, as studied in [35–38] does not affect the evolution of $\tilde{C}_p(t)$, since any momentum change due to the scattering or generation of Bogoliubov excitations acts as a projective measurement of the internal impurity state and can therefore not generate coherence.

The solution of Eq. (15) is readily obtained, and upon reintroducing the phase factor $\mathrm{e}^{i\varepsilon_\mathbf{p}t}$ gives

$$C_p(t) = \mathrm{e}^{-i(p^2/2m+n_\text{B}\mathcal{T}+\Sigma_p)t}\mathrm{e}^{i\int_0^t \mathrm{d}s\Gamma_p(s)}C_p(0), \tag{17}$$

with

$$\Sigma_p = n_\text{B}\mathcal{T}^2 \int \frac{\mathrm{d}^3k}{(2\pi)^3} g_\mathbf{k}^2 \left[\frac{\varepsilon_\mathbf{k}^\text{B}}{E_\mathbf{k}} \frac{1}{\varepsilon_\mathbf{p} - \varepsilon_{\mathbf{p}-\mathbf{k}} - E_\mathbf{k}} + \frac{2m_r}{k^2} \right]. \tag{18}$$

Here, we have used

$$\varepsilon_\mathbf{p} + \Gamma_p(0) = p^2/2m + n_\text{B}U_0 + \Gamma_p(0)$$
$$= p^2/2m + n_\text{B}\mathcal{T} + \Sigma_p \tag{19}$$

which follows from the Lippmann-Schwinger equation, relating U_0 to the zero-energy impurity-boson scattering matrix $\mathcal{T}$, as discussed in Sec. II. Equation (17) explicitly shows how the phase factor corresponding to the polaron energy $E_p = p^2/2m + n_\text{B}\mathcal{T} + \Sigma_p$ naturally emerges from our formalism. Indeed, Eq. (18) coincides with the second order contribution to the ground state energy of the Bose polaron obtained in [25, 28] in the limit of a zero range potential with $g_\mathbf{k} = 1$. Comparing Eq. (17) with the $t \to \infty$ limit given by Eq. (9), we see that the integral $\int_0^t \mathrm{d}s\Gamma_p(s)$ determines the dynamical formation of

the polaron state. Upon evaluating the integral in Eq. (16), the expression for $\Gamma_p(t)$ can be written as

$$\Gamma_p(t) = \Gamma \cdot \gamma(\alpha, p\xi/\sqrt{2}, t/t_{\mathrm{B}}), \qquad (20)$$

where

$$\Gamma = \frac{m_{\mathrm{B}}^2}{m_r^2} \frac{\sqrt{2}a^2}{a_{\mathrm{B}}\xi} t_{\mathrm{B}}^{-1}, \qquad (21)$$

is a rate constant, and $\gamma(\alpha, p\xi/\sqrt{2}, t/t_{\mathrm{B}})$ is a time dependent function that only depends on the mass ratio $\alpha = m/m_B$ and the dimensionless impurity momentum $p\xi/\sqrt{2}$ in units of the inverse of the BEC coherence length $\xi = 1/\sqrt{8\pi n_{\mathrm{B}}a_{\mathrm{B}}}$. Moreover, Eq. (21) contains the characteristic timescale $t_{\mathrm{B}} = \xi/\sqrt{2}c$ for the impurity dynamics, determined by the the speed of sound $c = \sqrt{4\pi n_{\mathrm{B}}a_{\mathrm{B}}}/m_{\mathrm{B}}$ of the condensate. This timescale reflects how fast Bogoliubov modes can build up distortions on a length scale ξ, which corresponds to the typical size of the formed screening cloud surrounding the impurity.

In Fig. 2, we display the time dependent rate coefficient $\Gamma_p(t)$ for different impurity momenta and fixed mass ratio $\alpha = m/m_B = 1$. As can be seen, the real part of $\Gamma_p(t)$ vanishes asymptotically for $t/t_{\mathrm{B}} \gg 1$ so that the phase factor of the coherence $\Gamma_p(t)$ approaches $\exp(-iE_p \cdot t)$ in the long time limit, in agreement with Eq. (9). We also see from Fig. 2 that the imaginary part of $\Gamma_p(t)$ vanishes for $t/t_{\mathrm{B}} \gg 1$ for impurity momenta below the Landau critical momentum $p_c = mc$ of the BEC. This reflects the infinite polaron lifetime $\tau_p \to \infty$, due to the absence of damping as it moves through the superfluid with $p < p_c$. However, when the impurity momentum exceeds p_c, Fig. 2 shows that the imaginary part of $\Gamma_p(t)$ approaches a finite value and yields a finite polaron lifetime τ_p due to the continual emission of Cherenkov radiation.

FIG. 2. (a) Real and (b) imaginary part of the rate coefficient, $\Gamma_p(t)$, as a function time, t, and impurity momentum, p. Times and momenta are scaled by $t_{\mathrm{B}} = \xi/\sqrt{2}c$ and $p_c = mc$, respectively, while $\Gamma_p(t)$ is shown in units of the rate constant Γ given in Eq. (21). The mass ratio is $\alpha = m/m_{\mathrm{B}} = 1$.

V. SHORT-TIME DYNAMICS AND THE ROLE OF THE INTERACTION RANGE

We begin by discussing the impurity dynamics due to decoherence at short times $t \ll t_{\mathrm{B}}$ prior to emergence of the polaron. To model a finite range impurity-boson interaction, we consider a simple step function in momentum space, $g_{\mathbf{k}} = \Theta(\kappa - k)$ where κ is a high momentum cut-off. This choice provides a simplified model for the actual interaction between the atoms, whose typical range, r_0, relates to the characteristic momentum $\kappa \sim r_0^{-1}$.

In Fig. 3, we plot the absolute value of the coherence for different values of the cut-off κ. As can be seen, the initial decoherence is characterised by a Gaussian damping $\ln|C_p(t)/C_p(0)| \sim -(t/t_i)^2$. The characteristic time for this initial decoherence is determined by the cut-off as $t_i \sim m_r/(\sqrt{n_{\mathrm{B}}}a\kappa^{3/2})$. This simple initial behavior applies for short times $t \lesssim m_r/\kappa^2$. Beyond this time, the decoherence proceeds in a way that is largely independent
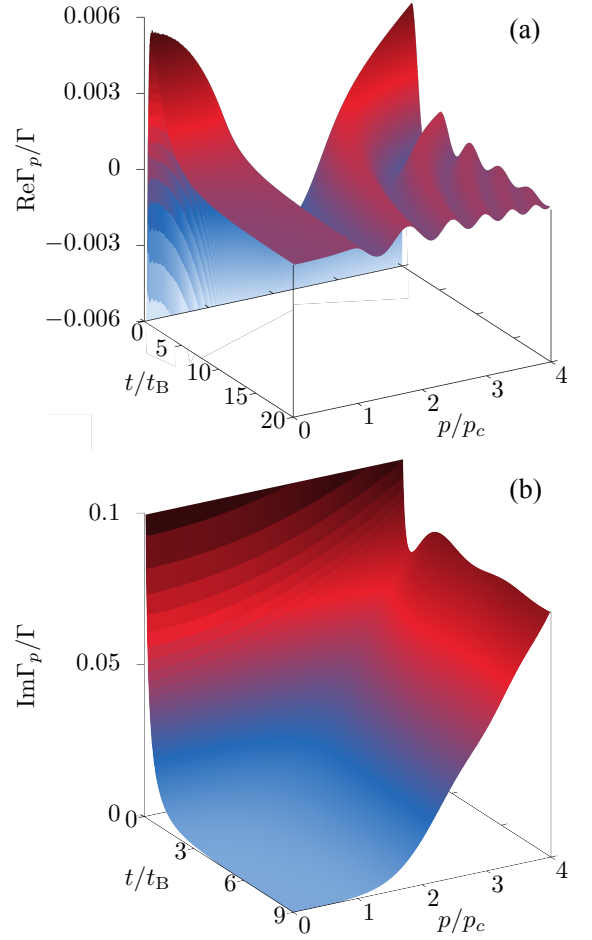
of κ. In fact, the characteristic extent of interactions between alkaline atoms is below 1nm and, thus, about two orders of magnitudes smaller than the typical coherence length $\xi \sim 0.1\mu$m of atomic BECs [40]. It follows that the initial Gaussian decoherence determined by the finite range of the interaction is only present at very short times. Under relevant experimental conditions, we can therefore neglect this initial Gaussian dynamics and take the zero-range limit $\kappa \to \infty$. In this limit, the rate $\Gamma_p(t)$ diverges at the initial time $t \to 0$. As shown in Fig. 3, this leads to fast initial decoherence but yields a well behaved coherence dynamics close to the results for finite values of $\kappa\xi \gg 1$.

To investigate this further, we plot in Fig. 4(a) the subsequent dynamics for different impurity momenta, p, and different values of the scattering length a. The initial decoherence appears to proceed independently of the impurity momentum, which can be readily understood from Eq. (16). At early times t, it takes large momenta k for the phase to rotate significantly in the exponential
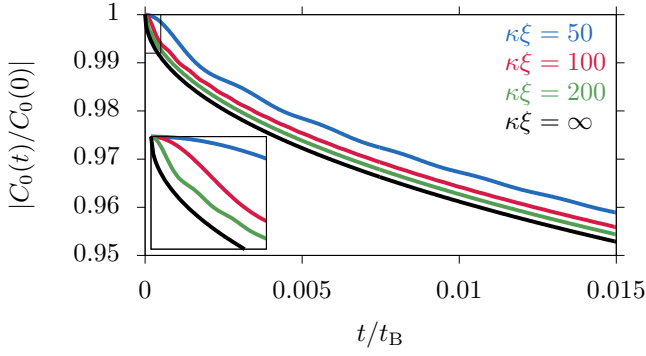
FIG. 3. Short-time behavior of the coherence for different indicated values of momentum scale κ that characterizes the range, $\sim 1/\kappa$, of the impurity-boson interaction potential. The inset illustrates the derived quadratic time dependence $\sim e^{-(t/t_i)^2}$ at very short times $t \lesssim m_r/\kappa^2$, where t_i scales as $t_i \sim 1/\kappa^{3/2}$ with κ. Beyond this initial time, however, all curves approach the universal decay law $|C_p| \sim e^{-\sqrt{t/t_0}}$ as demonstrated in the main panel. The remaining parameters are $\alpha = m/m_B = 1$, $a/\xi = 0.1$ and $a_B/\xi = 0.01$.

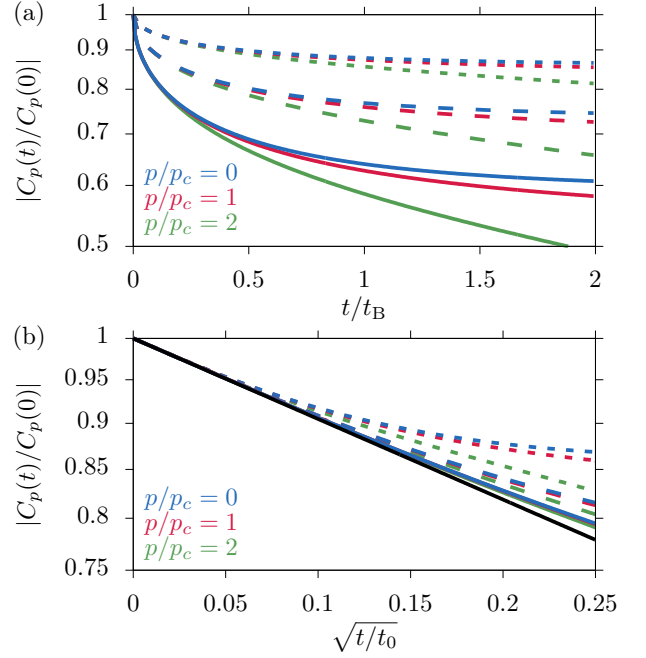
FIG. 4. Coherence dynamics for different indicated impurity momenta, p, and for different impurity-boson scattering lengths, $a/\xi = 0.07$ (dotted lines), $a/\xi = 0.1$ (dashed lines) and $a/\xi = 0.13$ (solid lines). For $t \lesssim t_B/2$, all of the different curves shown in panel (a) collapse to a single universal decay law $|C_p| \sim e^{-\sqrt{t/t_0}}$ [black line in (b)] as demonstrated in panel (b). The remaining parameters are $\alpha = m/m_B = 1$ and $a_B/\xi = 0.01$.

factor in the integrand for $\Gamma_p(t)$. The dominant contributions to the integral therefore stems from large momenta that eventually exceed the impurity momentum and render the initial decoherence of the impurity independent of p. In this regime, which is dominated by coupling to free-particle excitations, the initial impurity dynamics is also independent of the interaction among the condensate atoms, and only depends on the strength of their coupling to the impurity as parametrised by the scattering length a.

By expanding the integral for $\Gamma_p(t)$ in Eq. (16) for short times and evaluating the resulting integrals analytically, one can show that

$$C_p(t) = C_p(0)e^{i\left(p^2/2m + n_B \mathcal{T} t + \sqrt{t/t_0}\right) - \sqrt{t/t_0}}. \tag{22}$$

The appearing timescale is given by

$$t_0 = \frac{m_r}{16\pi n_B^2 a^4}, \tag{23}$$

which indeed only depends on a, the reduced mass m_r and the density whereas it is independent of p and a_B. Details of this derivation are given in App. F.

In Fig. 4(b), we plot the decoherence $|C_p(t)/C_p(0)|$ as a function of t/t_0 for the same momenta and scattering lengths as in Fig. 4(a). Indeed all data points collapse to a single curve given by Eq. (22) for times $t \lesssim t_B/2$. In the limit of an ideal Bose gas, the non-exponential decoherence given by Eq. (22) persists for all times, such that a polaron can consequently not be defined at any stage of the impurity dynamics. Thus, the decoherence initially follows a universal non-exponential relaxation $|C_p(t)| = |C_p(0)|e^{-\sqrt{t/t_0}}$, while the polaron properties,

such as the energy shift Σ_p and residue Z_p, have yet to emerge as we will discuss in the next section.

VI. LONG-TIME DYNAMICS

At later times, $t > t_B/2$, coupling to phonon modes starts to become significant and the coherence dynamics becomes dependent on the boson-boson interaction and the impurity momentum p. Asymptotically, the coherence approaches a finite steady state for $p < p_c$, while it continues to decay above the Landau critical momentum $p_c = mc$. This is illustrated in Fig. 5, showing how $|C_p(t)|$ relaxes to a constant value for $p < p_c$ but continues to decay exponentially for higher momenta. In this regime the dynamics is driven by phonon dressing leading to the eventual formation of the polaron, as we now demonstrate explicitly.

By evaluating the time dependent rate coefficient, Eq. (16), we can determine the asymptotic decay time $\tau_p = 1/[2\text{Im}\Gamma_p(\infty)]$ (see App. C)

$$\frac{1}{2\tau_p} = n_B \mathcal{T}^2 \int \frac{d^3k}{(2\pi)^3} \frac{\varepsilon_{\mathbf{k}}^B}{E_{\mathbf{k}}} \pi \delta(\varepsilon_{\mathbf{p}} - \varepsilon_{\mathbf{p-k}} - E_{\mathbf{k}}), \tag{24}$$
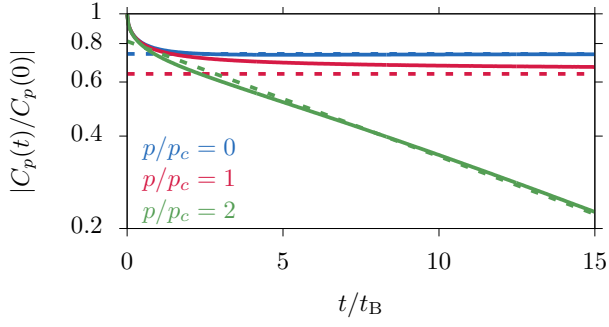
which coincides with the Fermi golden rule expression for

FIG. 5. Coherence dynamics for different indicated impurity momenta p. The solid lines show the derived solution of the master equation, which approaches the expected polaron steady state shown by the dashed lines. The depicted behavior indicates that the final approach towards this steady state becomes very slow for $p \approx p_c$. The remaining parameters are $\alpha = m/m_\mathrm{B} = 1$, $a_\mathrm{B}/\xi = 0.01$ and $a/\xi = 0.1$.

the spectral width of the polaron in equilibrium [25]. In Fig. 6 we show the instantaneous damping rate $\mathrm{Im}\Gamma_p(t)$. For $p < p_c$ the decay rate steadily decreases and vanishes at long times, reflecting the superfluidity of the condensate which leaves the eventually formed polaron state unaffected. For higher momenta, $p > p_c$, the impurity moves faster than the speed of sound and therefore emits Cherenkov phonon radiation, causing decoherence and exponential decay on a timescale of τ_p. We can separate this long time behavior in Eq. (17) such that

$$C_p(t) = \mathrm{e}^{-iE_p t - t/(2\tau_p)} \mathrm{e}^{\int_0^t \mathrm{d}s(i\Gamma_p(s) + 1/(2\tau_p))}.$$

Since the integral over the rate coefficient becomes purely imaginary at long times, we can use this expression to define the asymptotic quasiparticle residue

$$Z_p = \mathrm{e}^{-\int_0^\infty \mathrm{d}s(\mathrm{Im}\Gamma_p(s) - 1/(2\tau_p))}. \qquad (25)$$

As discussed further in App. D, this indeed coincides with the equilibrium result obtained in Ref. [28] from a diagrammatic expansion for zero momentum and
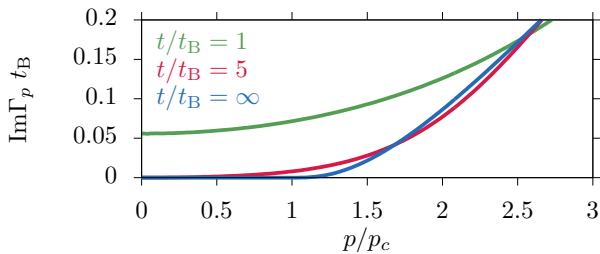

FIG. 6. Momentum dependence of the instantaneous damping rate $\mathrm{Im}\Gamma_p(t)$ at different indicated times in the impurity dynamics. For $p > p_c$ the impurity continues to decohere and therefore retains a finite decay rate, $1/\tau_p > 0$ as $t \to \infty$ (blue line). The remaining parameters are $\alpha = m/m_\mathrm{B} = 1$, $a/\xi = 0.1$ and $a_\mathrm{B}/\xi = 0.01$.
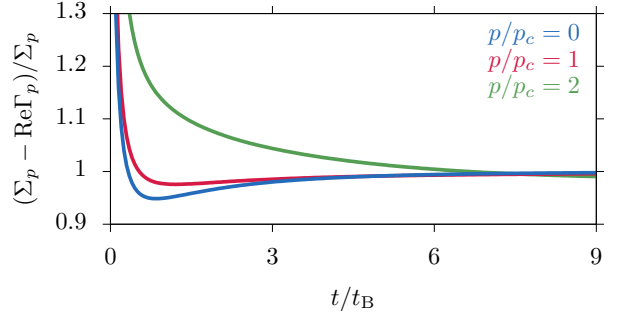

FIG. 7. Time dependence of the deviation $\Sigma_p - \mathrm{Re}\Gamma_p$ from the final polaron energy for different indicated impurity momenta p. Upon scaling energies by Σ_p and times by t_B, the depicted dynamics becomes independent of the scattering lengths. The used mass ratio is $\alpha = m/m_\mathrm{B} = 1$.

$a^2/(a_\mathrm{B}\xi) \ll 1$, and under more general conditions in Ref. [35].

Finally, we turn to the phase factor of the coherence. In Fig. 2 we saw that the real part of $\Gamma_p(t)$ vanishes asymptotically such that the phase factor of $C_p(t)$ approaches $\exp(-iE_p t)$. For $p = 0$ and $\alpha = 1$, the long-time phase rotation takes on a particularly simple form

$$\varepsilon_0 + \Sigma_0 - \mathrm{Re}\Gamma_0(t) = n_\mathrm{B}\mathcal{T} + \Sigma_0\left(1 - 45\frac{t_\mathrm{B}^4}{t^4}\right) \qquad (26)$$

where $\Sigma_0 = 32\sqrt{2}n_\mathrm{B}a^2/3m\xi$ for $\alpha = 1$ as obtained from Eq. (18) once more coincides with the expected equilibrium result, obtained for $p = 0$ and $a/\xi \ll 1$ [28]. While a more general expression for arbitrary momenta and mass ratios is derived in App. E, this simple result shows that one can define an asymptotic energy of the immersed impurity, which approaches the polaron ground state energy at long times. Equation (26) shows explicitly that the timescale for this approach is on the order of t_B for $\alpha = 1$ and zero momentum. As shown in Figs. 7 and 5, however, the corresponding characteristic timescale, t_f, for polaron formation can have a strong dependence of the impurity momentum, as we will discuss in the next section.

VII. POLARON FORMATION TIME

Below p_c, we find that the coherence always overshoots its eventual steady state. One can thus identify an intermediate relaxation stage (see Fig. 1), at the end of which the coherence, $|C_p(t)|$, goes through a minimum and the impurity starts its final approach to the polaron state. The location of this minimum can therefore be used to define the polaron formation time, t_f, which marks the onset of the final stage of the impurity dynamics. Since $\partial_t|C_p(t)| = -\mathrm{Im}\Gamma_p(t)|C_p(t)|$, this is equivalent to finding the first zero of $\mathrm{Im}\Gamma_p$, as illustrated in Fig. 8a.
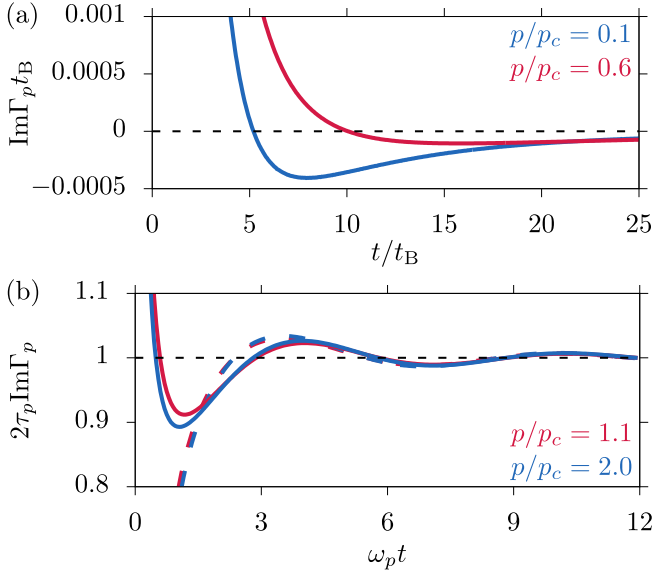
FIG. 8. Instanteneous damping rate $\mathrm{Im}\Gamma_p$ for different indicated impurity momenta p. The dashed lines show the expected asymptotic value $1/(2\tau_p)$, which vanishes below the critical momentum [panel (a)] but is finite for $p > p_c$ [panel (b)]. The used mass ratio is $\alpha = m/m_{\mathrm{B}} = 1$. For panel (a) we use $a/\xi = 0.1$, $a_{\mathrm{B}}/\xi = 0.01$.

We can capture the asymptotic coherence dynamics by expanding Eq. (16) in orders of $1/t$. As outlined in detail in App. E, this gives the following asymptotic behavior

$$\ln\left|\frac{C_p(t)}{C_p(0)}\right| = -\frac{a^2}{a_{\mathrm{B}}\xi}\left(A_p + B_p\frac{1}{(t/t_{\mathrm{B}})^2}\right). \quad (27)$$

where $\ln Z_p = -a^2/(a_{\mathrm{B}}\xi)A_p$, as shown in App. D. Both coefficients, A_p and B_p, depend only on the mass ratio, α, and the momentum ratio p/p_c. Regardless of these parameters, however, one finds that $B_p > 0$ is positive such that the coherence always approaches its final value from below. Since the coherence initially decreases, this implies that $|C_p(t)|$ indeed goes through a minimum for any $p < p_c$. Since, the expansion is only valid for $t \gg t_{\mathrm{B}}\sqrt{B_p/A_p}$ beyond t_{f}, we determine the formation time numerically. Interestingly, however, we find that the coefficient B_p diverges when the impurity momentum approaches p_c, indicating a logarithmic relaxation dynamics with a diverging formation time.

Above p_c, the formation time is also determined as the time when the rate first crosses its steady state value, which in this case corresponds to $\mathrm{Im}\Gamma_p(t_{\mathrm{f}}) = \frac{1}{2\tau_p}$. The final coherence dynamics exhibits damped oscillations which are well described by the asymptotic damping rate

$$\mathrm{Im}\Gamma_p(t) = \frac{1}{2\tau_p} + \frac{a^2}{a_{\mathrm{B}}\xi}D_p(\alpha)\frac{t_{\mathrm{B}}^{1/2}}{t^{3/2}}\cos\left(\omega_p t + \frac{\pi}{4}\right), \quad (28)$$

as derived in App. E. The coefficient D_p and the frequency ω_p only depend on α and the scaled impurity

momentum p/p_c. As shown in Fig. 8b, ω_p determines both the frequency as well as the amplitude damping of the oscillation, since scaling time by ω_p^{-1} renders the asymptotic coherence dynamics nearly independent of p. It is given by the simple relation

$$\omega_p = -\Delta E_{\mathbf{p},\mathbf{k}_0} = \varepsilon_{\mathbf{p}} - \varepsilon_{\mathbf{p}-\mathbf{k}_0} - E_{\mathbf{k}_0}, \quad (29)$$

which corresponds to the energy cost $\Delta E_{\mathbf{p},\mathbf{k}_0}$ associated with phonon generation, whereby the corresponding phonon momentum $\mathbf{k}_0$ lies at the stationary point

$$\nabla_{\mathbf{k}}\Delta E_{\mathbf{p},\mathbf{k}}|_{\mathbf{k}=\mathbf{k}_0} = 0 \quad (30)$$

that minimizes $\Delta E_{\mathbf{p},\mathbf{k}}$. This thus corresponds to energetic off-shell processes with phonon momenta around $\mathbf{k}_0$ where the phases in Γ_p add up constructively (see Eq. (16)), and which naturally cease to occur at large times $t \to \infty$ when off-shell scattering is suppressed by energy conservation.

In Fig. 9 we show our numerical results for t_{f} for equal masses $\alpha = 1$. In general we find that the formation decreases with α and eventually diverges as $\alpha \to 0$. This reflects the increasing effects of phonon recoil which tends to slow down the relaxation to a steady state. The found timescale for small momenta around $p = 0$ is consistent with the developed picture of polaron formation in terms of a phonon-induced decoherence process. It implies that the formation time corresponds to the time it takes to propagate the presence of the impurity. At zero momentum the size of the screening phonon cloud is on the order of the coherence length, ξ. Thus the expected formation time can be estimated by the time for a phonon to propagate this distance, $t_{\mathrm{f}} \sim \xi/c = \sqrt{2}t_{\mathrm{B}}$, which is consistent with the results shown in Fig. 9.

Most strikingly, we find that the formation time diverges when the impurity momentum approaches p_c from below as well as from above. At $p = p_c$ the coherence dynamics undergoes a critical slowdown and never reaches the polaron steady state as illustrated in Fig. 5. Close to
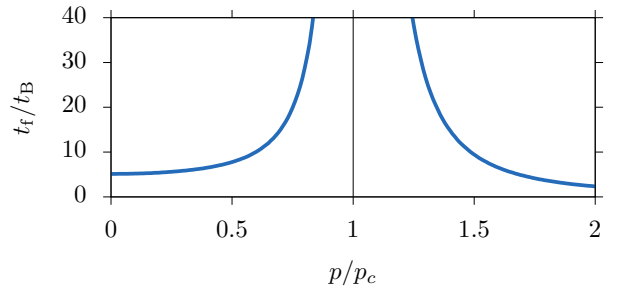

FIG. 9. Momentum dependence of the polaron formation time t_{f}. When scaled by t_{B} it does not depend on either scattering length and is a sole function of the impurity momentum and the mass ratio, which is chosen to be $\alpha = m/m_{\mathrm{B}} = 1$ in the figure. For $\alpha \le 1$ the formation time diverges as $(p - p_c)^{-2}$ on both sides of the singularity at $p = p_c$.

p_c the formation time can be described by the following critical behavior

$$t_{\rm f} = b \frac{t_{\rm B}}{|1 - p/p_c|^{\eta}}, \qquad (31)$$

where the proportionality constant b depends on the mass ratio. For $\alpha = 1$, the critical exponent is found to be $\eta = 2$ above and below p_c. This behavior can be understood as follows. As discussed above, the relevant timescale for the asymptotic approach to the polaron state above p_c is given by $1/\omega_p$. From Eqs. (29) and (30) one can show that $\omega_p t_{\rm B} = \alpha (p/p_c - 1)^2/4$ close to p_c (see App. E). Hence, we have a universal critical exponent of $\eta = 2$ for $p > p_c$. For $p < p_c$, on the other hand, the exponent turns out to depend on the mass ratio α. Explicitly, we find that for a light impurity with $\alpha \leq 1$ the critical exponent remains to be $\eta = 2$, while it acquires a mass dependence $\eta = 1 + (1 + 1/\alpha)/2$ for $\alpha \geq 1$.

Eq. (29) together with Eq. (30) shows that the oscillation and damping timescale above p_c is related to forward scattering of phonons with respect to the moving impurity. In fact, the same mechanism causes the divergence of B_p in Eq. (27), for $p < p_c$. When the impurity moves precisely at the speed of sound p_c/m, forward emitted phonons cannot dissipate away from the impurity as they propagate at the same velocity, rendering decoherence ineffective. Hence, forward scattering of phonons turns out to be the general bottleneck for the impurity relaxation and ultimately leads to the increasing polaron formation time when approaching the Landau critical momentum p_c.

VIII. CONCLUSION

In summary, we have studied the non-equilibrium dynamics of a quantum impurity immersed into a Bose-Einstein condensate. By tracing the dynamics of the impurity coherence via a master equation approach we could identify different dynamical regimes from an initially universal non-exponential coherence decay and a subsequent phonon-driven relaxation to the final formation of the polaron steady state. Considering different impurity momenta, we have found that the dynamical polaron formation undergoes a critical slowdown when approaching the Landau critical velocity of the condensate.

The thereby established link between the critical equilibrium properties of the condensate and the dynamical critical behavior of the non-equilibrium impurity state raises a number of open questions. For example it suggests that a similar slowdown might occur in condensates at finite temperature [47] and cause very long polaron formation times close to the critical temperature for Bose-Einstein condensation. Clarifying this open question should indeed be important for future experiments to study the Bose polaron at finite temperatures and across the BEC phase transition.

For the parameters of a recent experiment [20], in which Bose polarons have been created and studied by driving the $(F = 1, M_F = -1) \rightarrow (F = 1, m_F = 0)$ hyperfine transition of a ^{39}K BEC, we obtain for our relevant timescales $t_{\rm B} \approx 0.2$ms, $t_0 \approx 14$ms and $t_{\rm f} \approx 1$ms for $a = 20a_{\rm B}$ and $p = 0$. It turns out that the shortest timescale, $t_{\rm B} = 0.2$ms, is just about the duration of the microwave excitation pulse used in [20], such that the predictions of the present work should be observable with present technology. This would enable direct experimental access to the non-equilibrium properties of the Bose polaron.

The results of this work should also be relevant to other systems and similar problems, such as the decoherence of molecular rotational states in superfluid helium droplets [48], whose equilibrium properties have been linked to the quantum impurity physics in recent theoretical work [49–51]. Following these ideas, the theoretical framework described in the present work appears also applicable for the description of the short rotational dynamics of such molecules [48]. While the corresponding decoherence timescales are expected to be much shorter than for cold atom systems, they can be well resolved using fs-laser spectroscopy [48].

The formulated theory can also account for a finite range of the impurity interaction, which we used to demonstrate converged and well behaved dynamics in the limit of zero-range interactions in order to avoid ambiguities stemming from otherwise ad hoc momentum cutoffs. While the effects of a finite interaction range were shown to be small in typical alkaline atom BECs, they are most likely relevant for systems with larger interaction ranges, such as recently studied Rydberg state impurities [52], where it is possible to observe the initial impurity dynamics on timescales $t < t_i$ well before the polaron formation time $t_{\rm f} > t_i$.

The process of impurity decoherence is intrinsic to the formation of the polaron. Understanding its interplay with coherent driving of internal impurity states is important for the quality of light matter interfaces involving polaron physics. Examples include the fidelity of storage [53] and propagation [54] or quantum light coupled to atomic Rydberg excitations in the inevitable presence of interaction with their surrounding ground state atoms, Bose condensed atoms coupled to an optical cavity [55] for which the generation of dark-state polaritons has been suggested as a means to tune the effective polaron mass.

The derivation of rigorous analytical results and scaling relations has been made possible by focussing on the limit of weak impurity interactions. Yet, we expect several characteristics of the discussed impurity dynamics to survive under more general conditions. For example, the discovered critical slowdown of the polaron formation due to the discussed inhibition of phonon emission as well as the predicted universal short time behavior $|C_p(t)/C_p(0)| \approx 1 - \sqrt{t/t_0}$ should persist for stronger interactions and beyond the Fröhlich model for the Bose polaron.

Appendix A: The effective von Neumann equation

In this section we derive the effective von Neumann Eq. (13). We write the interaction Hamiltonian Eq. (1) in the interaction picture and the equation of motion for the impurity density operator after tracing over the bath and making the Born-Markov approximation (12)

$$H_{IB}(t) = \sum_{\mathbf{k},\mathbf{p}} U_{\mathbf{k}} \sqrt{\frac{n_B \varepsilon_{\mathbf{k}}^B}{V E_{\mathbf{k}}}} c_{\mathbf{p}-\mathbf{k}}^\dagger(t) c_{\mathbf{p}}(t) \left(\beta_{\mathbf{k}}^\dagger(t) + \beta_{-\mathbf{k}}(t) \right),$$

$$\partial_t \rho_I = -\int_0^t ds \mathrm{Tr}_B \left[H_{IB}(t), [H_{IB}(s), \rho_I(t) \otimes \rho_B(0)] \right].$$

Here $c_{\mathbf{p}}(t) = e^{-\varepsilon_p t} c_{\mathbf{p}}(0)$ and $\beta_{\mathbf{k}}(t) = e^{-iE_k t} \beta_{\mathbf{k}}(0)$ in the interaction picture. We then let $I_i(t) = c_{\mathbf{p}i-\mathbf{k}i}^\dagger(t) c_{\mathbf{p}i}(t)$ and $B_i(t) = \beta_{\mathbf{k}i}^\dagger(t) + \beta_{-\mathbf{k}i}(t)$ for $i = 1, 2$. Examining the commutator of the second line this yields terms like

$$\mathrm{Tr}_B[I_1(t) \otimes B_1(t), [I_2(s) \otimes B_2(s), \rho_I(t) \otimes \rho_B(0)]]$$
$$= \mathrm{Tr}\left(B_1(t) B_2(s) \right) [I_1(t), I_2(s)\rho_I(t)] +$$
$$\mathrm{Tr}\left(B_2(s) B_1(t) \right) [\rho_I(t) I_2(s), I_1(t)],$$

which can be calculated using only the identity $\mathrm{Tr}_B[I \otimes B] = I \ \mathrm{Tr}(B)$ for an impurity operator I and a bath operator B when tracing out the bath part. At zero temperature the density operator for the bath, the BEC, is simply: $\rho_B = |BEC\rangle \langle BEC|$. We then get $\mathrm{Tr}\left(B_1(t) B_2(s) \right) = \mathrm{Tr}\left(\beta_{-\mathbf{k}1}(t) \beta_{\mathbf{k}2}^\dagger(s) \right) = e^{-iE_{k1}t + iE_{k2}s} \langle BEC| \beta_{-\mathbf{k}1} \beta_{\mathbf{k}2}^\dagger |BEC\rangle = e^{-iE_k(t-s)} \delta_{-\mathbf{k}1,\mathbf{k}2}$, with $\mathbf{k} = \mathbf{k}_1$. We then get

$$\partial_t \rho_I = -\frac{n_B}{V} \int_0^t ds \sum_{\substack{\mathbf{k}1,\mathbf{k}2 \\ \mathbf{p}1,\mathbf{p}2}} U_{\mathbf{k}1} U_{\mathbf{k}2} \sqrt{\frac{\varepsilon_{\mathbf{k}1}^B \varepsilon_{\mathbf{k}2}^B}{E_{\mathbf{k}1} E_{\mathbf{k}2}}} \left(\mathrm{Tr} \beta_{-\mathbf{k}1}(t) \beta_{\mathbf{k}2}^\dagger(s) \right.$$
$$\times \left[c_{\mathbf{p}1-\mathbf{k}1}^\dagger(t) c_{\mathbf{p}1}(t), c_{\mathbf{p}2-\mathbf{k}2}^\dagger(s) c_{\mathbf{p}2}(s) \rho_I(t) \right] + \text{h.c.} \right)$$
$$= -\frac{n_B \mathcal{T}^2}{V} \int_0^t ds \sum_{\mathbf{k},\mathbf{p}1,\mathbf{p}2} g_{\mathbf{k}}^2 \frac{\varepsilon_{\mathbf{k}}^B}{E_{\mathbf{k}}} \left(e^{-iE_k(t-s)} \right.$$
$$\times \left[c_{\mathbf{p}1-\mathbf{k}}^\dagger(t) c_{\mathbf{p}1}(t), c_{\mathbf{p}2+\mathbf{k}}^\dagger(s) c_{\mathbf{p}2}(s) \rho_I(t) \right] + \text{h.c.} \right).$$

In the second equality we write $U_{\mathbf{k}} = U_0 g_{\mathbf{k}}$ and replace U_0 by the impurity-boson scattering matrix at zero energy $\mathcal{T} = 2\pi a/m_r$, with a the impurity-boson scattering length. This is consistent to second order in a. We hereby derived Eq. (13).

Appendix B: Analytical expression for Γ_0 in the equal mass case

We find a closed form expression for Γ_0. Using $\Phi_{\tilde{p}}(\tilde{k}) = -t_B(\varepsilon_{\mathbf{p}} - \varepsilon_{\mathbf{p}-\mathbf{k}} - E_{\mathbf{k}}) = \tilde{k}\sqrt{\tilde{k}^2 + 1} + \tilde{k}^2 - 2\tilde{k}\tilde{p}\cos(\theta)$, with $\tilde{k} = k\xi/\sqrt{2}$ and equal masses $m = m_B$ we write Eq. (16) of the main text on unitless form

$$\Gamma_p(\tilde{t}) t_B = -\frac{\sqrt{2}}{\pi} \frac{a^2}{a_B \xi} \int d\cos(\theta) d\tilde{k} \frac{\tilde{k}^3 e^{-i\Phi_{\tilde{p}}(\tilde{k})\tilde{t}}}{\sqrt{\tilde{k}^2 + 1} \Phi_{\tilde{p}}(\tilde{k})}, \quad (B1)$$

with $\tilde{t} = t/t_B$. Here $\cos\theta \in (-1,1)$ and $\tilde{k} \in (0,\infty)$. For zero impurity momentum, $p = 0$, Φ has the simple inverse: $\tilde{k} = \frac{\Phi}{\sqrt{1+2\Phi}}$. Using this we get

$$\Gamma_0(\tilde{t}) t_B = -\frac{2\sqrt{2}}{\pi} \frac{a^2}{a_B \xi} \int_0^\infty d\Phi \frac{\Phi^2}{(1+2\Phi)^{5/2}} e^{-i\Phi\tilde{t}}.$$

The problem has thus been reduced to calculating the above Fourier transform. A primitive to the integrand is found in Mathematica. With a bit of rewriting we then arrive at the result

$$\Gamma_0(\tilde{t}) t_B = -\frac{2\sqrt{2}}{\pi} \frac{a^2}{a_B \xi} \left[\frac{(1+i)\sqrt{\pi}}{24\sqrt{\tilde{t}}} \left(i\tilde{t}^2 + 6\tilde{t} - 3i \right) e^{i\tilde{t}/2} \right.$$
$$\times \left. \left(1 - \mathrm{erf}\left(\frac{1+i}{2} \sqrt{\tilde{t}} \right) \right) - \frac{5 + i\tilde{t}}{12} \right], \quad (B2)$$

with erf the error function. This has also been checked numerically. It is also possible to achieve an analytical expression for the integral of $\Gamma_0(t)$. Integrating (B2) we get

$$\int_0^t ds \, \Gamma_0(s) = \frac{\sqrt{2}}{3\pi} \frac{a^2}{a_B \xi} \left[\tilde{t} + i(i\tilde{t} + 3)\frac{1+i}{2}\sqrt{\pi\tilde{t}} \, e^{i\tilde{t}/2} \right.$$
$$\times \left. \left(1 - \mathrm{erf}\left(\frac{1+i}{2}\sqrt{\tilde{t}} \right) \right) \right]$$
$$\simeq i\frac{2\sqrt{2}}{3\pi} \frac{a^2}{a_B \xi} \left(1 + \frac{3}{\tilde{t}^2} \right), \quad (B3)$$

where the last expression is accurate asymptotically to order $\tilde{t}^{-2} = (t_B/t)^2$.

Appendix C: Damping in the long time limit

We calculate the polaron life-time, $1/2\tau_p = \lim_{t\to\infty} \mathrm{Im}\Gamma_p(t)$. We can write the damping as

$$\mathrm{Im}\Gamma_p(t) = n_B \mathcal{T}^2 \int \frac{d^3 k}{(2\pi)^3} \frac{\varepsilon_k^B}{E_k} \mathrm{Re} \int_0^t ds \, e^{+i(\varepsilon_{\mathbf{p}} - \varepsilon_{\mathbf{p}-\mathbf{k}} - E_{\mathbf{k}})s}.$$

For $t \to \infty$ the temporal integral yields $\int_0^\infty ds \, e^{+ixs} = \mathrm{Pr}(-i/x) + \pi\delta(x)$, where Pr stands for the principal value and $x = \varepsilon_{\mathbf{p}} - \varepsilon_{\mathbf{p}-\mathbf{k}} - E_{\mathbf{k}}$. Taking the real part of this expression gives the damping rate at long times

$$\mathrm{Im}\Gamma_p(\infty) = \frac{1}{2\tau_p} = n_B \mathcal{T}^2 \int \frac{d^3 k}{(2\pi)^3} \frac{\varepsilon_{\mathbf{k}}^B}{E_{\mathbf{k}}} \pi\delta(\varepsilon_{\mathbf{p}} - \varepsilon_{\mathbf{p}-\mathbf{k}} - E_{\mathbf{k}}),$$

with τ_p the polaron life-time. For momenta below the Landau critical momentum, $p < p_c = mc$, the integral is 0. For $p > p_c$ the integral can be evaluated analytically to yield

$$\frac{t_{\mathrm{B}}}{2\tau_p} = \frac{\alpha(1+1/\alpha)^2}{8\sqrt{2}} \frac{a^2}{a_{\mathrm{B}}\xi} \frac{\tilde{k}_{\max}\sqrt{1+\tilde{k}_{\max}^2} - \operatorname{arcsinh}(\tilde{k}_{\max})}{\tilde{p}}, \tag{C1}$$

for $p > p_c$, with $\tilde{p} = p\xi/\sqrt{2}$ and

$$\tilde{k}_{\max} = \frac{1}{\alpha^2 - 1}\left(\alpha\sqrt{(2\tilde{p})^2 + 1 - \alpha^2} - 2\tilde{p}\right), \tag{C2}$$

with $\tilde{k}_{\max} = \tilde{p} - \frac{1}{4\tilde{p}}$ in the equal mass case $\alpha = 1$. We hereby have a closed form expression for the long time damping for all mass ratios.

Appendix D: Momentum dependent residue

In this section we calculate the quasiparticle residue as given in Eq. (25)

$$Z_p = \mathrm{e}^{-\int_0^\infty \mathrm{d}t(\operatorname{Im}\Gamma_p(t) - 1/2\tau_p)}. \tag{D1}$$

Using that $\partial\Phi_{\tilde{p}}(\tilde{k})/\partial\cos(\theta) = -2\tilde{p}\tilde{k}/\alpha$ we can perform the angle integral in Eq. (B1) and get

$$\operatorname{Im}\Gamma_p(t)t_{\mathrm{B}} = \frac{\sqrt{2}(1+1/\alpha)^2}{4\pi} \frac{a^2}{a_{\mathrm{B}}\xi} \frac{\alpha}{2\tilde{p}} \int_0^\infty \mathrm{d}\tilde{k} \frac{\tilde{k}^2}{\sqrt{1+\tilde{k}^2}}$$
$$\times \left(\operatorname{Si}\left(\Phi_{\tilde{p}}^+(\tilde{k})\tilde{t}\right) - \operatorname{Si}\left(\Phi_{\tilde{p}}^-(\tilde{k})\tilde{t}\right)\right), \tag{D2}$$

with $\tilde{t} = t/t_{\mathrm{B}}$, $\tilde{k} = k\xi/\sqrt{2}$, $\alpha = m/m_{\mathrm{B}}$, $\operatorname{Si}(x) = \int_0^x \mathrm{d}u \sin(u)/u$ the sine integral, and $\Phi_{\tilde{p}}^\pm(\tilde{k}) = \tilde{k}\sqrt{\tilde{k}^2+1} + \frac{1}{\alpha}(\tilde{k}^2 \pm 2\tilde{k}\tilde{p})$. Then integrating the sine integrals we get

$$\int_0^t \mathrm{d}s\, \operatorname{Im}\Gamma_p(s) = \frac{\sqrt{2}(1+1/\alpha)^2}{4\pi} \frac{a^2}{a_{\mathrm{B}}\xi} \frac{\alpha}{2\tilde{p}} \int_0^\infty \mathrm{d}\tilde{k} \frac{\tilde{k}^2}{\sqrt{1+\tilde{k}^2}}$$
$$\times \left[\tilde{t}\left(\operatorname{Si}\left(\Phi_{\tilde{p}}^+(\tilde{k})\tilde{t}\right) - \operatorname{Si}\left(\Phi_{\tilde{p}}^-(\tilde{k})\tilde{t}\right)\right) + \right.$$
$$\left. \frac{\cos\left(\Phi_{\tilde{p}}^+(\tilde{k})\tilde{t}\right) - 1}{\Phi_{\tilde{p}}^+(\tilde{k})} - \frac{\cos\left(\Phi_{\tilde{p}}^-(\tilde{k})\tilde{t}\right) - 1}{\Phi_{\tilde{p}}^-(\tilde{k})}\right].$$

We recognise the first two terms in the integral as $\operatorname{Im}\Gamma_p(t)t$ which goes to $t/2\tau_p$ for $t \gg t_{\mathrm{B}}$. We therefore get

$$\ln Z_p = -\int_0^\infty \mathrm{d}s\left[\operatorname{Im}\Gamma_p(s) - \frac{1}{2\tau_p}\right]$$
$$= -\lim_{\tilde{t}\to\infty} \frac{\sqrt{2}(1+1/\alpha)^2}{4\pi} \frac{a^2}{a_{\mathrm{B}}\xi} \frac{\alpha}{2\tilde{p}} \int_0^\infty \mathrm{d}\tilde{k} \frac{\tilde{k}^2}{\sqrt{1+\tilde{k}^2}}$$
$$\times \left[\frac{\cos\left(\Phi_{\tilde{p}}^+(\tilde{k})\tilde{t}\right) - 1}{\Phi_{\tilde{p}}^+(\tilde{k})} - \frac{\cos\left(\Phi_{\tilde{p}}^-(\tilde{k})\tilde{t}\right) - 1}{\Phi_{\tilde{p}}^-(\tilde{k})}\right]$$
$$= -\frac{\sqrt{2}(1+1/\alpha)^2}{2\pi} \frac{a^2}{a_{\mathrm{B}}\xi} \operatorname{Pr}\int_0^\infty \mathrm{d}\tilde{k} \frac{\tilde{k}}{\sqrt{1+\tilde{k}^2}}$$
$$\times \frac{1}{\left(\sqrt{1+\tilde{k}^2} + \tilde{k}/\alpha\right)^2 - (2\tilde{p}/\alpha)^2}. \tag{D3}$$

In the second equality we use that $(\cos(\Phi\tilde{t}) - 1)/\Phi = -\int_0^{\tilde{t}} \mathrm{d}\tilde{s}\sin(\Phi\tilde{t}) = \operatorname{Im}\int_0^{\tilde{t}} \mathrm{d}\tilde{s}\exp(-i\Phi\tilde{t}) \to \operatorname{Pr}(-1/\Phi)$, for $\tilde{t} \to \infty$, with Pr the principal value. The resulting integral above can be readily be solved in the equal mass case $\alpha = 1$. Here, using $x = \sqrt{1+\tilde{k}^2} + \tilde{k}$ we get

$$\ln Z_p = -\frac{\sqrt{2}}{\pi} \frac{a^2}{a_{\mathrm{B}}\xi} \operatorname{Pr}\int_1^\infty \mathrm{d}x \frac{x^2 - 1}{x^2(x^2 - (2\tilde{p})^2)}$$
$$= -\frac{\sqrt{2}}{\pi} \frac{a^2}{a_{\mathrm{B}}\xi} \frac{1}{(2\tilde{p})^2}\left[1 + \frac{(2\tilde{p})^2 - 1}{2\tilde{p}}\operatorname{Re}\operatorname{arctanh}\left(\frac{1}{2\tilde{p}}\right)\right].$$

The integral is performed using the transformation $\tanh(\theta) = x/2\tilde{p}$. Note that $\operatorname{Re}\operatorname{arctanh}(1/x) = \operatorname{Re}\operatorname{arctanh}(x)$. The final result is then

$$\ln Z_p = -\frac{a^2}{a_{\mathrm{B}}\xi} \frac{\sqrt{2}}{\pi}\left(\frac{p_c}{p}\right)^2\left[1 + \frac{\left(\frac{p}{p_c}\right)^2 - 1}{p/p_c}\operatorname{Re}\operatorname{arctanh}\left(\frac{p}{p_c}\right)\right]$$
$$= -\frac{a^2}{a_{\mathrm{B}}\xi} A_p(1), \tag{D4}$$

thus defining $A_p(\alpha)$ for $\alpha = 1$. At $p = 0$ and $p = p_c$ a limiting process must be performed. We have thus obtained an analytical result for the residue as a function of momentum in the equal mass case. Below we give the limiting values of $A_p(\alpha)$ for general α calculated from Eq. (D3)

$$A_0(\alpha) = \frac{\sqrt{2}}{2\pi} \frac{\alpha+1}{\alpha-1}\left(1 - \frac{2}{\alpha+1}f(\alpha)\right),$$
$$A_{pc}(\alpha) = \frac{\sqrt{2}}{2\pi} \frac{\alpha+1}{\alpha-1}\ln\alpha, \tag{D5}$$

where $f(\alpha) = \sqrt{\frac{\alpha+1}{\alpha-1}}\arctan\sqrt{\frac{\alpha-1}{\alpha+1}}$ and $\sqrt{-1} = i$. Here $A_0(\alpha = 1) = 2\sqrt{2}/(3\pi)$

Appendix E: Asymptotic dynamics

In this section we calculate the asymptotic behavior of the coherence for general mass ratios, α, and momenta,

p. It turns out that there are two regimes in which this behaves quite differently: $p < p_c$ and $p > p_c$, where $p_c = mc$ is the Landau critical momentum of the condensate.

$\mathbf{p} < \mathbf{p_c}$: We calculate $\int_0^t ds \Gamma_p(s)$ to leading order in $1/t$. We will see that

$$\int_0^t ds \, \Gamma_p(s) \simeq \frac{a^2}{a_B\xi}\left(A_p(\alpha) + B_p(\alpha)\left(\frac{t_B}{t}\right)^2\right), \quad (E1)$$

where $A_p(\alpha)$ is defined in Eq. (D4). This analysis is detailed below.

For reference we write Eq. (16) of the main text on unitless form ($\alpha = m/m_B$)

$$\Gamma_p(t) = -\frac{\sqrt{2}(1+1/\alpha)^2}{4\pi t_B}\frac{a^2}{a_B\xi}\int d\cos\theta d\tilde{k}\frac{\tilde{k}^3 e^{-i\Phi_{\tilde{p}}(\tilde{k})\tilde{t}}}{\sqrt{1+\tilde{k}^2}\Phi_{\tilde{p}}(\tilde{k})}$$

$$= -\frac{\sqrt{2}(1+1/\alpha)^2}{4\pi t_B}\frac{a^2}{a_B\xi}\int d\cos\theta d\tilde{k} \, w_{\tilde{p}}(\tilde{k}) e^{-i\Phi_{\tilde{p}}(\tilde{k})\tilde{t}},$$
$$(E2)$$

where $\Phi_{\tilde{p}}(\tilde{k}) = \tilde{k}\sqrt{\tilde{k}^2+1} + (\tilde{k}^2 - 2\tilde{k}\tilde{p}\cos\theta)/\alpha$, and $\tilde{k} = k\xi/\sqrt{2}$. Here $\cos\theta \in (-1,1)$ and $\tilde{k} \in (0,\infty)$. The second equality defines $w_{\tilde{p}}(\tilde{k}) = \tilde{k}^3/(\sqrt{\tilde{k}^2+1}\Phi_{\tilde{p}}(\tilde{k}))$. We now wish to expand the integral asymptotically for $\tilde{t} = t/t_B \gg 1$. Specifically we investigate the $\tilde{k}$-integral and write

$$I_\theta = \int d\tilde{k} \, w_{\tilde{p}}(\tilde{k}) e^{-i\Phi_{\tilde{p}}(\tilde{k})} = \frac{1}{-i\tilde{t}}\int d\tilde{k}\frac{w_{\tilde{p}}(\tilde{k})}{\partial_{\tilde{k}}\Phi_{\tilde{p}}}\partial_{\tilde{k}}e^{-i\Phi_{\tilde{p}}(\tilde{k})\tilde{t}},$$

which is a simple rewritting valid as long as $\partial_{\tilde{k}}\Phi_{\tilde{p}} \neq 0$ for all $\tilde{k}$. This turns out to be the case as long as we are below the critical momentum, $p < p_c = mc$, or in units of ξ: $\tilde{p} = p\xi/\sqrt{2} < \alpha/2$. Then since the integral is now written as a function times the derivate of another we can use integration by parts. Repeating this procedure successively gives a systematic asymptotic expansion in powers of $1/\tilde{t}$. It turns out that we have to go to order $1/\tilde{t}^3$ to get a nonzero contribution

$$I_\theta = -\frac{i}{\tilde{t}^3}\frac{\partial_{\tilde{k}}\left(\frac{\partial_{\tilde{k}}(w_{\tilde{p}}/\partial_{\tilde{k}}\Phi_{\tilde{p}})}{\partial_{\tilde{k}}\Phi_{\tilde{p}}}\right)}{\partial_{\tilde{k}}\Phi_{\tilde{p}}}e^{-i\Phi_{\tilde{p}}(\tilde{k})\tilde{t}}\Bigg|_{\tilde{k}=0}^{\tilde{k}=\infty} + \mathcal{O}\left(\frac{1}{\tilde{t}^4}\right)$$

$$= \frac{i}{\tilde{t}^3}\frac{2}{(1-2\tilde{p}/\alpha\cos\theta)^4} + \mathcal{O}\left(\frac{1}{\tilde{t}^4}\right).$$

In the second equality we use that at low $\tilde{k}$ the functions asymptotically behave like $w_{\tilde{p}}(\tilde{k}) \to k^2/(1-2p/\alpha\,\cos\theta)$ and $\partial_{\tilde{k}}\Phi_{\tilde{p}} \to 1 - 2p/\alpha\,\cos\theta$. Inserting this in Eq. (E2), and performing the angle integral we then get the asymp-

tote

$$\text{Im}\Gamma_p(t)t_B \simeq -\frac{1}{\tilde{t}^3}\frac{\sqrt{2}(1+1/\alpha)^2}{6\pi}\frac{a^2}{a_B\xi}\frac{\alpha}{2\tilde{p}}$$
$$\times\left(\frac{1}{(1-2\tilde{p}/\alpha)^3} - \frac{1}{(1+2\tilde{p}/\alpha)^3}\right).$$

Integrating this and using $\int_0^\infty ds \, \text{Im}\Gamma_p(s) = A_p(\alpha)\times a^2/(a_B\xi)$ we get

$$\int_0^t ds \, \text{Im}\Gamma_p(s) = \int_0^\infty ds \, \text{Im}\Gamma_p(s) - \int_t^\infty ds \, \text{Im}\Gamma_p(s)$$

$$\simeq \frac{a^2}{a_B\xi}\left[A_p(\alpha) + \left(\frac{t_B}{t}\right)^2\frac{\sqrt{2}(1+1/\alpha)^2}{12\pi}\frac{p_c}{p}\right.$$

$$\left.\times\left(\frac{1}{(1-p/p_c)^3} - \frac{1}{(1+p/p_c)^3}\right)\right].$$

In the first line we use $\tilde{t} = t/t_B$, $\tilde{p} = p\xi/\sqrt{2}$, and $p_c\xi/\sqrt{2} = \alpha/2$. Comparing with Eq. (E1) we get

$$B_p(\alpha) = \frac{\sqrt{2}(1+1/\alpha)^2}{12\pi}\frac{p_c}{p}\left(\frac{1}{(1-p/p_c)^3} - \frac{1}{(1+p/p_c)^3}\right).$$
$$(E3)$$

Further, taking the $p = 0$ limit in the above, we get $B_0(\alpha = 1) = 2\sqrt{2}/\pi$. This fits perfectly with the asymptotic form derived from an analytical expression for the integral in Eq. (B3), which serves as a good check of our current expression. We have also successfully checked the asymptote numerically. This asymptotic expansion is accurate for $t/t_B \gg \sqrt{B_p/A_p}$. Evaluating I_θ to fourth order yields the dominant contribution to $\text{Re}\Gamma$ at long times

$$\text{Re}\Gamma_p(t) \simeq \left(\frac{t_B}{t}\right)^4\frac{3\sqrt{2}(1+1/\alpha)^2}{2\pi\alpha t_B}\frac{a^2}{a_B\xi}\frac{p_c}{p}\times$$
$$\left(\frac{1}{(1-p/p_c)^5} - \frac{1}{(1+p/p_c)^5}\right) \quad (E4)$$

$\mathbf{p} > \mathbf{p_c}$: A key feature for the above calculation is that the phase $\Phi_{\tilde{p}}(\tilde{k})$ has no *stationary* point, i.e. $\partial_{\tilde{k}}\Phi_{\tilde{p}} \neq 0$ for all $\tilde{k}$. For $p > p_c$ this is no longer true. As we shall now see, this leads to a different asymptotic behavior of Γ_p.

The strategy in this case is slightly different. We take Eq. (D2) and use the large argument asymptote of the sine integral $\text{Si}(x) \simeq \pi/2 - \cos(x)/x$

$$\text{Im}\Gamma_p(t)t_B \sim \frac{\sqrt{2}(1+1/\alpha)^2}{4\pi}\frac{a^2}{a_B\xi}\frac{\alpha}{2\tilde{p}}\int d\tilde{k}\frac{\tilde{k}^2}{\sqrt{1+\tilde{k}^2}}$$
$$\left(\frac{\cos(\Phi_{\tilde{p}}^-(\tilde{k})\tilde{t})}{\Phi_{\tilde{p}}^-(\tilde{k})\tilde{t}} - \frac{\cos(\Phi_{\tilde{p}}^+(\tilde{k})\tilde{t})}{\Phi_{\tilde{p}}^+(\tilde{k})\tilde{t}}\right), \quad (E5)$$

The phase $\Phi_{\tilde{p}}^-(\tilde{k})$ has a stationary point $\tilde{k}_0$, i.e. $\partial_{\tilde{k}}\Phi_{\tilde{p}}^-|_{\tilde{k}=\tilde{k}_0} = 0$ defined by the equation $0 = \sqrt{\tilde{k}_0^2 + 1} +$

$\tilde{k}_0^2/\sqrt{\tilde{k}_0^2+1}+2(\tilde{k}_0-\tilde{p})/\alpha$. At the end of this section we will calculate $\tilde{k}_0$ in the limit $p \gtrsim p_c$. In general it turns out however, that this equation is quite involved to solve. Because of this stationary point the term in Eq. (E2) corresponding to Φ^- contains the leading order contribution at long times. We let $w_{\tilde{p}}^-(\tilde{k}) = \tilde{k}^2/(\sqrt{1+\tilde{k}^2}\Phi_{\tilde{p}}^-(\tilde{k}))$ and calculate the integral

$$
\begin{aligned}
I_- &= \int_0^\infty d\tilde{k}\, w_{\tilde{p}}^-(\tilde{k}) e^{-i\Phi_{\tilde{p}}^-(\tilde{k})\tilde{t}} \\
&\simeq e^{-i\Phi_{\tilde{p}}^-(\tilde{k}_0)\tilde{t}} \int_{-\infty}^\infty d\tilde{k}\, w_{\tilde{p}}^-(\tilde{k}) e^{-i\Phi_{\tilde{p}}''/2\,(k-k_0)^2\tilde{t}} \\
&\simeq e^{-i\Phi_{\tilde{p}}^-(\tilde{k}_0)\tilde{t}} w_{\tilde{p}}^-(\tilde{k}_0)\sqrt{\frac{2\pi}{\Phi_p''\tilde{t}}} e^{i\pi/4}.
\end{aligned}
$$

First we expand the phase to second order in $\tilde{k}-\tilde{k}_0$: $\Phi_{\tilde{p}}^-(\tilde{k}) \simeq \Phi_{\tilde{p}}^-(\tilde{k}_0) + \Phi_p''(k-k_0)^2/2$. This is valid to do at long times, because away from $\tilde{k}_0$ the heavy oscillations lead to rapid cancellation. We also use this to expand the integral to $-\infty$. We use the rapid cancellation simply to evaluate the function in front at $\tilde{k}=\tilde{k}_0$. Finally, we evaluate the integral in the last step. Taking the real part of I_- and dividing by $\tilde{t}$ we get the leading order contribution to the damping we were after

$$
\begin{aligned}
\mathrm{Im}\Gamma_p &\simeq \frac{1}{2\tau_p} + \frac{(1+1/\alpha)^2}{2\sqrt{\pi}} \frac{a^2}{a_B\xi} \frac{t_B^{1/2}}{t^{3/2}} \frac{p_c}{p} \frac{w_{\tilde{p}}^-(\tilde{k}_0)}{\sqrt{\Phi_{\tilde{p}}''}} \\
&\quad \times \cos\left(\Phi_{\tilde{p}}^-(\tilde{k}_0)t/t_B + \pi/4\right) \\
&= \frac{1}{2\tau_p} + \frac{a^2}{a_B\xi} D_p(\alpha) \frac{t_B^{1/2}}{t^{3/2}} \cos\left(\omega_p t + \pi/4\right). \quad (E6)
\end{aligned}
$$

Here we have included the nonzero damping rate found in Eq. (C1), which the stationary phase approximation fails to calculate. We also define the expansion coefficient, D_p and frequency of oscillation, ω_p according to

$$
\begin{aligned}
D_p(\alpha) &= \frac{(1+1/\alpha)^2}{2\sqrt{\pi}} \frac{p_c}{p} \frac{w_{\tilde{p}}^-(\tilde{k}_0)}{\sqrt{\Phi_{\tilde{p}}''}}, \\
\omega_p &= \Phi_{\tilde{p}}^-(\tilde{k}_0)/t_B. \quad (E7)
\end{aligned}
$$

Numerically, we have found that this expansion works very well after a few oscillations: $\omega_p t > 1$. Remember that $\partial_{\tilde{k}}\Phi_{\tilde{p}}^-|_{\tilde{k}=\tilde{k}_0} = 0$ and that $\mathbf{k}_0$ is parallel to $\mathbf{p}$ in Φ^-. This explicitly shows that ω_p is the energy difference of the impurity before and after it has emitted a phonon in the forward direction. Further, this is at the minimum of the energy difference. For $p \to p_c^+$, $k_0 = \alpha(p/p_c-1)/2$ and in turn $\omega_p t_B = \alpha(p/p_c-1)^2/4$.

Appendix F: Short-time behavior of $\Gamma_p(t)$

In this section we calculate the short-time behavior of $\Gamma_p(t)$ for all momenta p and mass ratios α. We further use this to calculate the coherence for short times and in the ideal Bose gas limit, $a_B \to 0$.

We wish to expand Eq. (E2) at short times $\tilde{t} = t/t_B \ll 1$. Now we infer a large momentum $\Lambda \gg \sqrt{2}/\xi$. We initially assume that we are at sufficiently short times so that for $\tilde{k} \le \tilde{\Lambda} = \Lambda\xi/\sqrt{2}$: $\Phi_{\tilde{p}}(\tilde{k})\tilde{t} \ll 1$. By expanding the exponential in the above integral we then get the following low momentum contribution

$$
I_p^{\mathrm{low}}(t) = \int \cos\theta \int_0^{\tilde{\Lambda}} d\tilde{k} \frac{\tilde{k}^3}{\sqrt{1+\tilde{k}^2}} \left[\frac{1}{\Phi_{\tilde{p}}(\tilde{k})} - i\tilde{t}\right]. \quad (F1)
$$

It is clear that this integral contains contributions of $\mathcal{O}(1)$ and $\mathcal{O}(\tilde{t})$. Further, for $\tilde{k} > \tilde{\Lambda} \gg 1$ we can approximate the phase as $\Phi_{\tilde{k}}(\tilde{p}) = \tilde{k}\sqrt{\tilde{k}^2+1} + (\tilde{k}^2 - 2\tilde{k}\tilde{p}\cos\theta)/\alpha \simeq \tilde{k}^2(1+1/\alpha)$. Inserting this into Eq. (E2) for $k > \Lambda$, we get the high momentum contribution

$$
\begin{aligned}
I^{\mathrm{high}}(t) &= \int d\cos\theta \int_{\tilde{\Lambda}}^\infty d\tilde{k} \frac{\tilde{k}^3}{\sqrt{1+\tilde{k}^2}} \frac{e^{-i\Phi_{\tilde{p}}(\tilde{k})\tilde{t}}}{\Phi_{\tilde{p}}(\tilde{k})} \\
&\simeq \frac{2}{1+1/\alpha} \int_{\tilde{\Lambda}}^\infty d\tilde{k}\, e^{-i(1+1/\alpha)\tilde{k}^2\tilde{t}},
\end{aligned}
$$

which is independent of the impurity momentum, p. The integral is readily evaluated using the identity $\mathrm{erfi}(x) = -i\,\mathrm{erf}(ix) = 2/\sqrt{\pi}\int_0^x du\, e^{u^2}$ for the imaginary error function erfi. Explicitly, we get

$$
\begin{aligned}
I^{\mathrm{high}}(t) &= -\frac{2}{1+1/\alpha} \frac{1+i}{2\sqrt{2}} \sqrt{\frac{\pi}{(1+1/\alpha)\tilde{t}}} \\
&\quad \times \mathrm{erfi}\left(\frac{i-1}{\sqrt{2}}\sqrt{(1+1/\alpha)\tilde{t}}\,\tilde{k}\right)\Bigg|_{\tilde{k}=\tilde{\Lambda}}^{\tilde{k}=\infty} \\
&= \frac{2}{1+1/\alpha}\left[\frac{1-i}{2\sqrt{2}}\sqrt{\frac{\pi}{(1+1/\alpha)\tilde{t}}} - \tilde{\Lambda}\right]. \quad (F2)
\end{aligned}
$$

Here we expand the primitive at the lower limit $\tilde{k} = \tilde{\Lambda}$ to lowest non-vanishing order in $\tilde{t}$. Adding the low and high momentum parts, neglecting the term of $\mathcal{O}(\tilde{t})$, and with a bit of rewriting, we get

$$
\begin{aligned}
\Gamma_p(t) &= \frac{\sqrt{2}(1+1/\alpha)^2}{4\pi t_B} \frac{a^2}{a_B\xi} \int d\cos\theta \int_0^{\tilde{\Lambda}} d\tilde{k}\left[-\frac{\tilde{k}^3}{\sqrt{1+\tilde{k}^2}}\right. \\
&\quad \times \left.\frac{1}{\Phi_{\tilde{p}}(\tilde{k})} + \frac{1}{1+1/\alpha}\right] - \frac{1}{4t_B}\sqrt{\frac{1+1/\alpha}{\pi}} \frac{a^2}{a_B\xi} \frac{1-i}{\sqrt{\tilde{t}}} \\
&= \Sigma_p - \frac{1}{4t_B}\sqrt{\frac{1+1/\alpha}{\pi}} \frac{a^2}{a_B\xi}(1-i)\sqrt{\frac{t_B}{t}}. \quad (F3)
\end{aligned}
$$

Λ now takes on the role of an initial momentum cut-off. The initial expansion, Eq. (F1), only works for finite Λ, but the above expression is valid for $t \ll t_B$ for any large value of Λ. Importantly, we recognize the integral as the second order polaron energy shift, Σ_p, which is independent of Λ as long as it is sufficiently high. As for the integral of Γ_p we get to linear order in t

$$\int_0^t \mathrm{d}s\, \Gamma_p(s) \simeq (i-1)\sqrt{\frac{t}{t_0}} + \Sigma_p t, \qquad \text{(F4)}$$

where we define $1/t_0 = 16\pi n_{\mathrm{B}}^2 a^4/m_r$. The coherence at short times is then

$$C_p(t) = C_p(0)\mathrm{e}^{-i(p^2/2m+n_{\mathrm{B}}\mathcal{T}+\Sigma_p)t}\mathrm{e}^{i\int_0^t \mathrm{d}s\Gamma_p(s)}$$
$$\simeq C_p(0)\mathrm{e}^{-i(p^2/2m+n_{\mathrm{B}}\mathcal{T})t}\mathrm{e}^{-(1+i)\sqrt{t/t_0}}, \qquad \text{(F5)}$$

which explicitly shows that the coherence does not depend on the polaron energy at short times, only the overall mean-field shift $n_{\mathrm{B}}\mathcal{T}$ is present. Also, the decay of $|C_p(t)|$ is independent of momentum. As noted in the main text when we approach the ideal Bose gas limit, $a_{\mathrm{B}} \to 0$, the coherence collapses to this short-time behavior for all times.

[1] E. Altman, in *Strongly Interacting Quantum Systems out of Equilibrium: Lecture Notes of the Les Houches Summer School*, Vol. 99, edited by T. Giamarchi, A. J. Millis, O. Parcollet, H. Saleur, and L. F. Cugliandolo (Oxford University Press, Oxford, 2016) arXiv:1512.00870.

[2] C. Chin, R. Grimm, P. Julienne, and E. Tiesinga, Rev. Mod. Phys. **82**, 1225 (2010).

[3] M.-S. Heo, T. T. Wang, C. A. Christensen, T. M. Rvachov, D. A. Cotta, J.-H. Choi, Y.-R. Lee, and W. Ketterle, Phys. Rev. A **86**, 021602 (2012).

[4] C.-H. Wu, J. W. Park, P. Ahmadi, S. Will, and M. W. Zwierlein, Phys. Rev. Lett. **109**, 085301 (2012).

[5] I. Bloch, J. Dalibard, and W. Zwerger, Rev. Mod. Phys. **80**, 885 (2008).

[6] T. Esslinger, Annual Review of Condensed Matter Physics **1**, 129 (2010), https://doi.org/10.1146/annurev-conmatphys-070909-104059.

[7] P. Bordia, H. Lüschen, S. Scherg, S. Gopalakrishnan, M. Knap, U. Schneider, and I. Bloch, Phys. Rev. X **7**, 041047 (2017).

[8] P. W. Anderson, Phys. Rev. **109**, 1492 (1958).

[9] L. Fleishman and P. W. Anderson, Phys. Rev. B **21**, 2366 (1980).

[10] L. D. Landau, Phys. Z. Sowjetunion **3**, 644 (1933).

[11] G. Mahan, *Many-Particle Physics* (Kluwer Academic/Plenum Publishers, 2000).

[12] A. Schirotzek, C.-H. Wu, A. Sommer, and M. W. Zwierlein, Phys. Rev. Lett. **102**, 230402 (2009).

[13] C. Kohstall, M. Zaccanti, M. Jag, A. Trenkwalder, P. Massignan, G. M. Bruun, F. Schreck, and R. Grimm, Nature **485**, 615 EP (2012).

[14] M. Koschorreck, D. Pertot, E. Vogt, B. Fröhlich, M. Feld, and M. Köhl, Nature **485**, 619 EP (2012).

[15] M. Cetina, M. Jag, R. S. Lous, I. Fritsche, J. T. M. Walraven, R. Grimm, J. Levinsen, M. M. Parish, R. Schmidt, M. Knap, and E. Demler, Science **354**, 96 (2016).

[16] F. Scazza, G. Valtolina, P. Massignan, A. Recati, A. Amico, A. Burchianti, C. Fort, M. Inguscio, M. Zaccanti, and G. Roati, Phys. Rev. Lett. **118**, 083602 (2017).

[17] F. Chevy and C. Mora, Reports on Progress in Physics **73**, 112401 (2010).

[18] P. Massignan, M. Zaccanti, and G. M. Bruun, Reports on Progress in Physics **77**, 034401 (2014).

[19] R. Schmidt, M. Knap, D. A. Ivanov, J.-S. You, M. Cetina, and E. Demler, Reports on Progress in Physics **81**, 024401 (2018).

[20] N. B. Jørgensen, L. Wacker, K. T. Skalmstang, M. M. Parish, J. Levinsen, R. S. Christensen, G. M. Bruun, and J. J. Arlt, Phys. Rev. Lett. **117**, 055302 (2016).

[21] M.-G. Hu, M. J. Van de Graaff, D. Kedar, J. P. Corson, E. A. Cornell, and D. S. Jin, Phys. Rev. Lett. **117**, 055301 (2016).

[22] J. Tempere, W. Casteels, M. K. Oberthaler, S. Knoop, E. Timmermans, and J. T. Devreese, Phys. Rev. B **80**, 184504 (2009).

[23] S. P. Rath and R. Schmidt, Phys. Rev. A **88**, 053632 (2013).

[24] W. Li and S. Das Sarma, Phys. Rev. A **90**, 013618 (2014).

[25] W. Casteels and M. Wouters, Phys. Rev. A **90**, 043602 (2014).

[26] J. Levinsen, M. M. Parish, and G. M. Bruun, Phys. Rev. Lett. **115**, 125302 (2015).

[27] L. A. P. Ardila and S. Giorgini, Phys. Rev. A **92**, 033612 (2015).

[28] R. S. Christensen, J. Levinsen, and G. M. Bruun, Phys. Rev. Lett. **115**, 160401 (2015).

[29] L. A. P. Ardila and S. Giorgini, Phys. Rev. A **94**, 063640 (2016).

[30] E. Compagno, G. De Chiara, D. G. Angelakis, and G. M. Palma, Scientific Reports **7**, 2355 (2017).

[31] F. Grusdt, R. Schmidt, Y. E. Shchadilova, and E. Demler, Phys. Rev. A **96**, 013607 (2017).

[32] A. Camacho-Guardian, L. A. P. Ardila, T. Pohl, and G. M. Bruun, ArXiv e-prints (2017), arXiv:1804.00402 [cond-mat.quant-gas].

[33] S. M. Yoshida, S. Endo, J. Levinsen, and M. M. Parish, Phys. Rev. X **8**, 011024 (2018).

[34] Y. E. Shchadilova, R. Schmidt, F. Grusdt, and E. Demler, Phys. Rev. Lett. **117**, 113002 (2016).

[35] A. Shashi, F. Grusdt, D. A. Abanin, and E. Demler, Phys. Rev. A **89**, 053617 (2014).

[36] F. Grusdt, K. Seetharam, Y. Shchadilova, and E. Demler, Phys. Rev. A **97**, 033612 (2018).

[37] T. Lausch, A. Widera, and M. Fleischhauer, ArXiv e-prints (2017), arXiv:1708.09242 [cond-mat.quant-gas].

[38] A. Lampo, C. Charalambous, M. Ángel García-March, and M. Lewenstein, ArXiv e-prints (2018), arXiv:1803.08946 [cond-mat.quant-gas].

[39] Y. Ashida, R. Schmidt, L. Tarruell, and E. Demler, Phys. Rev. B **97**, 060302 (2018).

[40] C. J. Pethick and H. Smith, *Bose-Einstein condensation in dilute gases*, Vol. 2nd edition (Cambridge University Press, 2008).

[41] H. Fröhlich, Proceedings of the Royal Society of London. Series A, Mathematical and Physical Sciences **215**, 291 (1952).

[42] M. Cetina, M. Jag, R. S. Lous, J. T. M. Walraven, R. Grimm, R. S. Christensen, and G. M. Bruun, Phys. Rev. Lett. **115**, 135302 (2015).

[43] M. Cetina, M. Jag, R. S. Lous, I. Fritsche, J. T. M. Walraven, R. Grimm, J. Levinsen, M. M. Parish, R. Schmidt, M. Knap, and E. Demler, Science **354**, 96 (2016).

[44] F. Schmidt, D. Mayer, Q. Bouton, D. Adam, T. Lausch, N. Spethmann, and A. Widera, ArXiv e-prints (2018), arXiv:1802.08702 [cond-mat.quant-gas].

[45] H.-P. Breuer and F. Petruccione, *The theory of open quantum systems* (Oxford University Press, 2002).

[46] H.-P. Breuer, D. Burgarth, and F. Petruccione, Phys. Rev. B **70** (2004).

[47] N.-E. Guenther, P. Massignan, M. Lewenstein, and G. M. Bruun, Phys. Rev. Lett. **120**, 050405 (2018).

[48] D. Pentlehner, J. H. Nielsen, A. Slenczka, K. Mølmer, and H. Stapelfeldt, Phys. Rev. Lett. **110**, 093002 (2013).

[49] R. Schmidt and M. Lemeshko, Phys. Rev. Lett. **114**, 203001 (2015).

[50] M. Lemeshko, Phys. Rev. Lett. **118**, 095301 (2017).

[51] G. Bighin and M. Lemeshko, Phys. Rev. B **96**, 085410 (2017).

[52] F. Camargo, R. Schmidt, J. D. Whalen, R. Ding, G. Woehl, S. Yoshida, J. Burgdörfer, F. B. Dunning, H. R. Sadeghpour, E. Demler, and T. C. Killian, Phys. Rev. Lett. **120**, 083401 (2018).

[53] I. Mirgorodskiy, F. Christaller, C. Braun, A. Paris-Mandoki, C. Tresp, and S. Hofferberth, Phys. Rev. A **96**, 011402 (2017).

[54] J. D. Thompson, T. L. Nicholson, Q.-Y. Liang, S. H. Cantu, A. V. Venkatramani, S. Choi, I. A. Fedorov, D. Viscor, T. Pohl, M. D. Lukin, and V. Vuletić, Nature **542**, 206 EP (2017).

[55] F. Grusdt and M. Fleischhauer, Phys. Rev. Lett. **116**, 053602 (2016).